Theoretical study of corundum as an ideal gate dielectric material for graphene transistors

Bing Huang, Qiang Xu, and Su-Huai Wei

Phys. Rev. B **84**, 155406 — Published 7 October 2011

DOI: 10.1103/PhysRevB.84.155406

Theoretical Study of Corundum as an Ideal Gate Dielectric Material for Graphene Transistors

Bing Huang, Qiang Xu, and Su-Huai Wei
National Renewable Energy Laboratory, 1617 Cole Boulevard, Golden, CO 80401, USA
(Dated: September 26, 2011)

Using physical insights and advanced first-principles calculations, we suggest that corundum (α-Al_2O_3) is an ideal gate dielectric material for graphene transistors. Clean interface exists between graphene and Al-terminated (or hydroxylated) Al_2O_3 and the valence band offsets for these systems are large enough to create injection barrier. Remarkably, a band gap of $\sim$ 180 meV can be induced in graphene layer adsorbed on Al-terminated surface with an electron effective mass of $\sim 8 \times 10^{-3}$ m_e. Moreover, the band gaps of graphene/Al_2O_3 system could be tuned by an external electric field for practical applications.

PACS numbers: 73.22.-f, 68.65.Pq, 68.43.Bc, 68.47.Gh

I. INTRODUCTION

Graphene has been studied intensively due to its unique electronic and mechanical properties such as extremely high carrier mobility (over 200000 $cm^2/V{\cdot}s$ for suspended samples)[1]. However, to utilize graphene, which has a zero band gap when it is pure, for electronic devices such as the field-effect transistors (FETs), it is essential to open up a band gap in graphene to realize the ON/OFF switch function. One way to open the band gap in graphene is utilizing the quantum confinement effect, e.g., etching graphene into one-dimensional nanoribbons[2–5]. In experiments, extremely narrow graphene nanoribbons (GNRs) ($\sim$ 10 nm) are necessary to achieve a band gap of $\sim$ 0.2 eV (ON/OFF ratio $> 10^2$)[3–5], but a large scale production of such narrow GNRs is still quite challenging. Moreover, the carrier mobility of GNRs (about hundreds of $cm^2/V{\cdot}s$[4, 5]) is several magnitudes lower than that of graphene sheet due to the (intrinsic) band folding and phonon scattering[6] as well as (extrinsic) difficulty in controlling the edge quality in experiments[4, 5]. Another way to open a band gap in graphene is breaking the inversion symmetry of the A, B sublattices, e.g., by placing graphene onto some special substrate. In this case, the band structure near the Dirac point or the carrier mobility of the graphene is better preserved if the interaction between graphene and substrates is weak. Obviously, this approach has technological advantages over the etching of graphene. However, a simple guideline on how to search an ideal substrate that could induce a sufficiently large band gap in graphene is still unclear, especially for substrate which can be integrated directly into the current FET technology.

Most of the graphene FETs to date employ silicon oxide (SiO_2) as the bottom-gate dielectric and an alternative high-dielectric-constant (high-k) material as the top-gate dielectric (e.g., the amorphous structures of HfO_2[7] and Al_2O_3[8]). The integration of a high-k top-gate can push the FET performance to a much higher limit because it can better screen charged impurities and enhance carrier mobility in graphene[7–9]. Analogy to silicon FET, an optimal high-k gate dielectric material should have high dielectric constant, large injection barrier (i.e., large band offset (> 1 eV) with respect to graphene), high chemical stability, and no or minimal interface states at the high-k-oxide/graphene interface[10]. In addition, an ideal high-k dielectric is desired to have the ability to open an adequate gap in graphene for FET operation.

Although several calculations have shown that a small gap could be induced in graphene by SiO_2[11, 12], HfO_2[13], or h-BN[14] substrates, a general rule to find a substrate which can induce a larger band gap in graphene is still lacked. Here, we propose that one should search for the substrate which has atoms with large chemical potential difference at the surface and is commensurate with the graphene lattice. These two conditions can cause large potential difference Δ_{AB} at the A, B sublattices of graphene, thus produce large band gap in graphene. Under this physical insight, we suggest that the (reconstructed) Al-terminated α-Al_2O_3 (0001) surface is an ideal high-k-oxide substrate for graphene FETs. This is because after the reconstruction both Al and O are present at the surface and the chemical potential difference between Al and O is much larger than that of other popular substrates such as SiO_2, h-BN, and HfO_2 studied before, and the lattice mismatch between α-Al_2O_3 (0001) and graphene is also relatively small. Carried out by advanced first-principles calculations, we demonstrate that a large band gap of $\sim$ 180 meV at the Dirac point appears in graphene layer adsorbed on Al-terminated (0001) surface with a quite small effective mass of $\sim 8 \times 10^{-3}$ m_e for Dirac fermions. As we expected, the band gap of graphene on Al_2O_3 is significantly larger than on other widely used substrates[15]. The size of the band gaps of graphene/Al_2O_3 systems could be further tuned by an external electric field for practical applications. Moreover, interface states can be eliminated if graphene is grown on Al-terminated (or hydroxylated) Al_2O_3 (0001) surface and the valence band offsets for these hybrid systems are large enough for injection barrier.

II. COMPUTATIONAL METHODS AND MODELS

All the density-functional-theory (DFT) calculations are performed by using the VASP code[16]. Projector augmented wave (PAW) potentials are used to describe the core electrons, and generalized gradient approximation (GGA) with the PBE functional is selected in our calculations. We find that the van de Waals (vdW) interaction plays an indispensable role in accurately determining the adsorption configuration and binding strength in this system. The effect of vdW interactions is taken into account by using the empirical correction scheme of Grimme (DFT + D/PBE)[17], which has been proved to be successful in describing the geometries of graphene related structures[18]. Our DFT+D/PBE calculations show that the interlayer distance of graphite is 3.22 Å and the interlayer binding energy is -54 meV/C-atom, in excellent agreement with quantum Monte Carlo calculation (-56 meV/C-atom)[19] and experimental value (-52±5 meV/C-atom)[20]. It is well-known that GGA type calculations usually underestimate the band gaps of semiconductors and the absolute band edge energy from the GGA calculation is not always reliable. Since hybrid functional calculations could give improved results for both conventional semiconductors[21] and graphene nanostructures[22], we adopt HSE hybrid functional to calculate the electronic structures of these Al_2O_3/graphene systems. The Al_2O_3 (0001) surface is modeled by a slab containing six oxygen O_3 layers and twelve

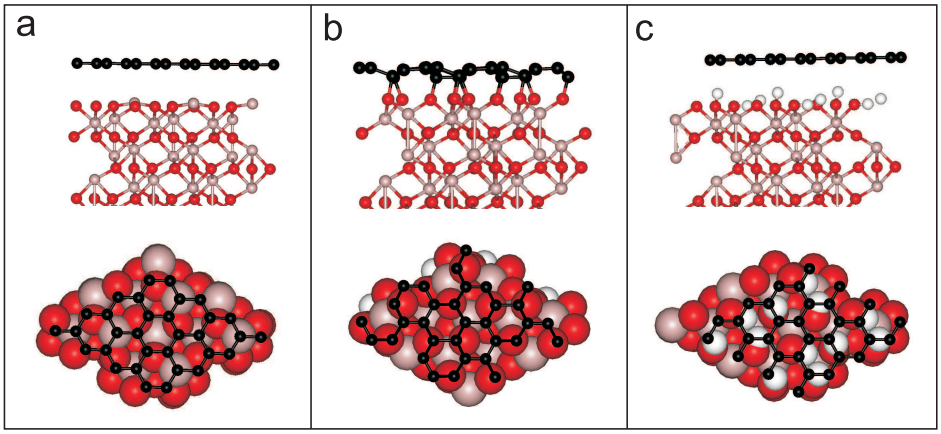

FIG. 1: (Color online) Side and top views of optimized structures of graphene on (a) Al-terminated, (b) O-terminated, and (c) fully hydroxylated Al_2O_3 (0001) surface. The black, red (dark gray) and pink (light gray) balls denote the C, O and Al atoms, respectively.

or eleven aluminum layers (depending on the specific surface studied). The second surface of the slab is passivated by pseudo H atoms[23] and a 15 Å-vacuum region is included. Single-layer or bilayer graphene with 2×2 periodicity is placed on 1×1 cell of Al_2O_3 with a lattice mismatch ∼2%[24]. A Γ-centered $24 \times 24 \times 1$ **k**-point sampling is used for the Brillouin-zone integration. The energy cutoff is set to 400 eV and structural optimization is carried out on all systems until the residual forces are converged to 0.01 eV/Å. The dipolar correction has been included[25].

III. RESULTS AND DISCUSSION

α-Al_2O_3 has rhombohedral symmetry $R\bar{3}c$ (D^6_{3d}, No. 167). The oxygen atoms form a nearly hcp structure, and the metal atoms fill two-thirds of the octahedral sites between the oxygen layers[26]. The (0001) surface of α-Al_2O_3 is of major technology importance because it is often used as a substrate in growth of semiconducting as well as superconducting materials. Low-energy electron diffraction (LEED) revealed that the (0001) crystal surface exhibits a 1×1 structure below ∼1250° in air or in vacuum[26–28]. Although theoretical calculations demonstrated that Al-terminated (0001) surface is the most stable one[29, 30], both Al- and O- terminated (0001) surfaces are observed in experiments and considered in our present work[26–28].

For the Al-terminated (0001) surface, our calculations show that the topmost Al atoms move down ∼ 0.65 Å into the next oxygen layer after the relaxation compared to the cleaved surface, as shown in Fig. 1a. This surface reconstruction stabilizes the surface by the large suppression of surface polarization[29, 30]. In order to investigate the stable interface structures, we have calculated all the high symmetrical arrangements between graphene and Al-terminated surface, where a surface Al or O atom is directly below either: a graphene C atom (T_{Al} or T_O), the hollow site of graphene C atoms (H_{Al} or H_O), or the center of C-C bridge site (B_{Al} or B_O). In addition, the case of a C atom directly above the center of surface Al-O bridge site is also considered. Our DFT+D/PBE total energy calculations indicate that the most stable configuration is the T_{Al} (Fig. 1a) with an adsorption energy of -76.4 meV/C-atom and the distance between graphene layer and substrate surface is ∼ 2.74 Å. The adsorption energy of the T_{Al} configuration is more negative than other high symmetrical configurations by 2 ∼ 9 meV/C-atom. It should be noticed that the vdW correction is very important in this case: without the vdW correction, the calculated interface distance of the T_{Al} configuration would be drastically increased to 3.31 Å and the adsorption energy would be only -2.6 meV/C-atom; the energy difference between T_{Al} and other configurations is within 2 meV/C-atom in the absence of vdW correction. LDA calculation could give a similar interlayer distance between graphene and substrate surface, but the binding energy is still largely underestimated by 34 meV/C-atom. Therefore, previous results on graphene weak adsorption on various substrates by LDA (or GGA) calculations[11–14] should be carefully reconsidered.

On the O-terminated surface, as each O atom has one dangling bond, the O-terminated surface is chemically reactive and could strongly interact with the graphene layer[31]. For the lowest energy configuration, all three surface O atoms in the unit cell form chemical bonds with the graphene layer to suppress the surface dangling bonds, as shown in Fig. 1b. The C-O bond length ranges from 1.45 to 1.50 Å. These C-O binding severely distort the planar graphene structure (C-C bond length varies from 1.36 to 1.49 Å) and the binding energy between graphene and O-terminated surface is -349 meV/C-atom, which is much larger than that of Al-terminated surface. In addition,

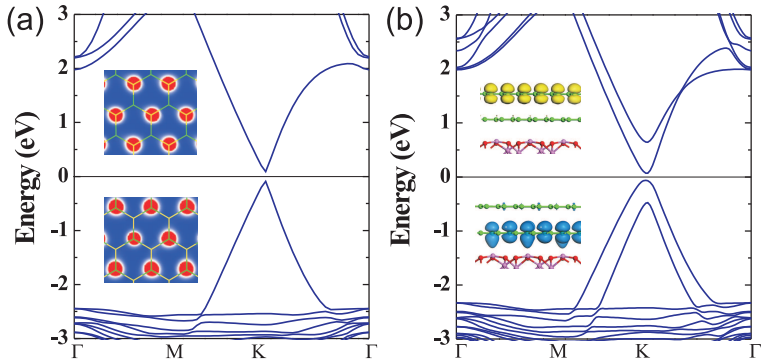

FIG. 2: (Color online) HSE functional calculated electronic band structures of (a) single-layer graphene and (b) bilayer graphene on Al-terminated (0001) Al_2O_3 surface. The Fermi level is set to zero. The partial charge densities of VBM and CBM for the two structures are plotted as bottom and upper insets in (a) and (b), respectively.

fully hydroxylated Al_2O_3 surface is also considered, as H atoms can be incorporated into the bulk structure during growth[26]. Previous calculations also demonstrated that the stability of fully hydroxylated surface is comparable to the Al-terminated one and much more stable than O-terminated surface[29, 30]. Similar to Al-terminated surface, graphene layer adsorbed on hydroxylated surface also belongs to vdW interaction. The most stable configuration is B_O (one surface O directly below the center of C-C bridge site), as shown in Fig. 1c. The interlayer distance between graphene layer and hydroxylated surface ranges from 2.31 Å to 3.18 Å due to the rippled structure at the interface and the binding energy is -49.2 meV/C-atom, slightly smaller than the binding strength of interlayers in graphite. The binding energy of B_O case is slightly lower than that of T_O and H_O within 1 meV/C-atom, indicating that these configurations are almost degenerate in energy.

After knowing the stable interface structures, we turn to understand the effects of Al_2O_3 substrate on the electronic property of graphene. The HSE band structure of single-layer graphene adsorbed on Al-terminated surface (T_{Al} configuration) is shown in Fig. 2a. Notably, the degeneracy of Dirac cone of graphene is lifted and a band gap of 182 meV (69 meV in DFT+D/PBE calculations) appears at the Fermi level, generating an effective mass of the Dirac fermions $\sim 8 \times 10^{-3}$ m_e. This is because the inversion symmetry in the graphene plane is broken on Al_2O_3 surface so the A, B sublattices, which is equivalent in free-standing graphene, is no longer equivalent. We find that the electrostatic potential difference of graphene C atoms at the A and B site differ by $\sim$ 165 meV, close to the value of the band gap, and this value is much larger than graphene on SiO_2[11, 12], HfO_2[13], and h-BN[14]. The charge density distributions of conduction band minimum (CBM) and valence band maximum (VBM) (inset of Fig. 2a) are found separately located in the different A and B sublattices of graphene layer, which is consistent with our explanation.

The sizes of band gaps of graphene in other high symmetrical configurations are close to that of T_{Al}, indicating that a similar ON/OFF ratio could be obtained even if graphene slides away from its ground state T_{Al} configuration. Remarkably, the band gap of graphene on Al-terminated Al_2O_3 is comparable to 10-nm-width GNRs in experiments[3–5]. Meanwhile, the effective mass of carriers in graphene/Al_2O_3 is an order lower than that of GNRs (~ 0.07 m_e) from theoretical calculation[32], strongly indicating the much higher carrier mobility of graphene/Al_2O_3 in practice. The band alignment between the graphene and substrate surface is found to be type-I and there are no interface states around Fermi level for the Al-terminated interface (Fig. 2a). By distinguishing the respective graphene and Al_2O_3 states, we can calculate the band offset for this hybrid system. The valence band offset between graphene and Al_2O_3 is about 2.35 eV from the hybrid functional calculation (DFT+D/PBE level calculation seriously underestimates the valence band offset by 1 eV), comparable to that of silicon and Al_2O_3[10], which is high enough for injection barrier.

The electronic properties of bilayer graphene on Al-terminated surface, as shown in Fig. 2b. The equilibrium graphene interlayer distance with AB stacking is 3.18 Å. Similar to single-layer graphene, a band gap of 138 meV is induced in bilayer graphene due to the inversion symmetry breaking. The VBM and CBM are contributed by A_1 and B_2 sublattices (A_1 and B_1 belong to the bottom layer while A_2 and B_2 belong to the top layer) in different graphene layers, respectively, as shown in Fig. 2b. The valence band offset between bilayer graphene and Al_2O_3 is 2.26 eV, slightly smaller than that of single-layer graphene. As we expected, the band gap of graphene on Al_2O_3 is significantly larger than that on other popular substrates such as SiO_2, HfO_2, and h-BN, indicating that α-Al_2O_3 is a better choice for gate material[15].

The electronic properties of graphene on O-terminated surface are completely different from that of Al-terminated one. Due to the strong interaction between graphene and surface O atoms, the linear band characteristic of graphene disappears, as shown in Fig. 3a. The gap states in Fig. 3a originate from the hybridization between graphene C

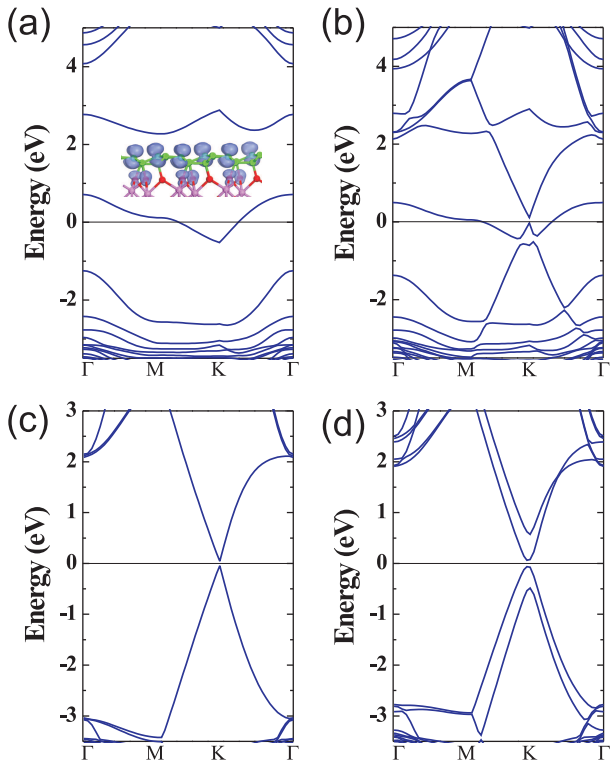

FIG. 3: (Color online) HSE functional calculated electronic band structures of (a) single-layer graphene and (b) bilayer graphene on O-terminated (0001) Al_2O_3 surface; the partial charge densities of the partially occupied band at the Fermi level in (a) are plotted as inset. HSE electronic band structures of (c) single-layer graphene and (d) bilayer graphene on fully hydroxylated (0001) Al_2O_3 surface are also plotted. The Fermi level is set to zero.

orbitals and surface O orbitals, shown as the inset in Fig. 3a. When a second graphene layer is placed on the surface (the graphene interlayer distance varies from 3.09 Å to 3.75 Å due to the rippled structure of the bottom layer), these gap states couple with the second layer graphene states and perturb its linear band distribution, as shown in Fig. 3b. A band gap of 140 meV appears for the second graphene layer, but the interface states exist inside the gap. Because these localized interface states can largely suppress the high mobility of graphene, O-terminated surface must be avoided to contact with graphene when gating graphene in experiments.

The electronic properties of graphene adsorbed on hydroxylated surface show similar behaviors to the Al-terminated surface, as shown in Figs. 3c and 3d for B_O configuration. No interface states around Fermi level are found and a band gap of 84 meV is induced in graphene layer with the effective mass of $\sim 4 \times 10^{-3}$ m_e for the Dirac fermion. The valence band offset between graphene and hydroxylated surface is 3.39 eV, larger than that of Al-terminated one. Moreover, the electronic properties of T_O and H_O configurations are quite similar to that of B_O. Comparing to the single layer case, the bilayer graphene on the hydroxylated surface has a larger band gap of 126 meV and smaller band offset of 3.24 eV, as shown in Fig. 3d. Clearly, O-terminated surface should be hydroxylated in order to make clean interface between graphene and Al_2O_3. Although the amorphous structure of Al_2O_3 has been selected as a top gate in some experiments[8], it is difficult for us to directly compare our results with these experiments due to the different phases.

Finally, we considered the electronic properties of graphene/Al_2O_3 hybrid system under an external electric field (E_{ext}) to simulate the gating effect in experiments[25]. Taking graphene on Al-terminated surface as examples, Fig. 4 shows the band gap and valence band offset of graphene/Al_2O_3 system as a function of E_{ext}. For single-layer graphene on Al_2O_3, a negative E_{ext} increases the band gap while the trend is opposite for a positive E_{ext}, as shown in Fig. 4a. This is because a positive (negative) E_{ext} increases (decreases) the distance between graphene and surface, e.g., the distance increases (decreases) from 2.74 Å to 2.86 (2.69) Å when E_{ext} = 0.6 (-0.6) V/Å. The increase of the distance between graphene and substrate reduces the potential difference $\triangle_{AB}$, thus changing the band gap. The variation of potential difference also influences the valence band offset, as shown in Fig. 4. The valence band offset increases (decreases) with a negative (positive) E_{ext} and varies from 2.49 eV to 2.05 eV under -0.6 eV/Å$\leq E_{ext} \leq$ 0.6 eV/Å.

The situation is quite different for bilayer graphene/Al_2O_3 (Fig. 4b) under an E_{ext}. Due to the symmetry, the band gap of bilayer graphene is determined mainly by the absolute difference of $|\triangle_{A_1B_2}|$.[33] This value reaches minimum

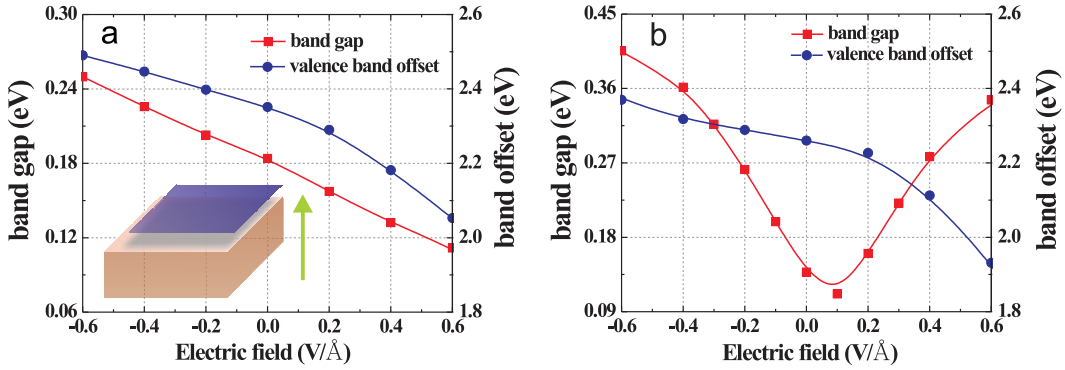

FIG. 4: (Color online) HSE functional calculated band gap and valence band offset of (a) single-layer graphene and (b) bilayer graphene on Al-terminated Al_2O_3 surface as a function of external electric field (E_{ext}). The principal scheme of the computational model is shown as inset of (a). An E_{ext} is oriented normally to a surface and is assumed to be positive when it is directed upward.

at $E_{ext} \sim 0.1$ V/Å when the system has a minimum anticrossing band gap around 112 meV. As E_{ext} increases or decreases from this value, $|\triangle_{A_1B_2}|$ increases, which makes the band gap increases as well, as shown in Fig. 4b. For example, the band gap of bilayer graphene increases to 361 meV at E_{ext} = -0.4 V/Å. The valence band offset changes between 2.37 eV and 1.93 eV for -0.6 eV/Å$\leq E_{ext} \leq$ 0.6 eV/Å. Thus, even under high E_{ext}, the valence band offset (injection barrier) of graphene/Al_2O_3 is still large enough.

IV. SUMMARY

With physical insights and by first-principles calculations we demonstrate that α-Al_2O_3 is an ideal high-k gate material for graphene FETs. There are no interface states between graphene and Al-terminated or hydroxylated Al_2O_3 surface and the valence band offset for this hybrid system is larger than 2 eV. Remarkably, a band gap of $\sim$ 180 meV appears in graphene layer deposited on Al-terminated surface, which is significantly larger than on other popular used substrates. Furthermore, the band gap of graphene/Al_2O_3 system could be tuned by an external electric field for practice applications.

Acknowledgments

The authors thank the helpful discussions with Dr. Zuanyi Li (UIUC), Dr. Junyi Zhu (NREL), and Prof. Jaejun Yu (SNU). The work at NREL was supported by the U.S. Department of Energy under Contract No. DE-AC36-08GO28308.

[1] A. K. Geim and K. S. Novoselov, Nature Mater. **6**, 183 (2007); A. H. Castro Neto, F. Guinea, N. M. R. Peres, K. S. Novoselov, and A. K. Geim, Rev. Mod. Phys. **81**, 109 (2009).
[2] Q. Yan, B. Huang, J. Yu, F. Zheng, J. Zhang, J. Wu, B. -L. Gu, F. Liu, and W. H. Duan, Nano Lett. **7**, 1469 (2007).
[3] M. Y. Han, B. Ozyilmaz, Y. Zhang, and P. Kim, Phys. Rev. Lett. **98**, 206805 (2007).
[4] X. Li, X. Wang, L. Zhang, S. Lee, and H. Dai, Science **319**, 1229 (2008).
[5] X. Wang, Y. Ouyang, X. Li, H. Wang, J. Guo, and H. Dai, Phys. Rev. Lett. **100**, 206803 (2008).
[6] A. Betti, G. Fiori, and G. Iannaccone, Appl. Phys. Lett. **98**, 212111 (2011).
[7] K. Zou, X. Hong, D. Keefer, and J. Zhu, Phys. Rev. Lett. **105**, 126601 (2010).
[8] L. Liao, J. Bai, Y. Qu, Y. Huang, and X. Duan, Nanotechnology **21**, 015705 (2010); S. Kim, J. Nah, I. Jo, D. Shahrjerdi, L. Colombo, Z. Yao, E. Tutuc, and S. K. Banerjee, Appl. Phys. Lett. **94**, 062107 (2009).
[9] C. Jang, S. Adam, J.-H. Chen, E. D. Williams, S. Das Sarma, and M. S. Fuhrer, Phys. Rev. Lett. **101**, 146805 (2008).
[10] H. J. Xiang, L. F. Da Silva, H. M. Branz, and S. -H. Wei, Phys. Rev. Lett. **103**, 116101 (2009).
[11] Y. Kang, J. Kang, and K. J. Chang, Phys. Rev. B **78**, 115404 (2008).
[12] N. T. Cuong, M. Otani, and S. Okada, Phys. Rev. Lett. **106**, 106801 (2011).
[13] K. Kamiya, N. Umezawa, and S. Okada, Phys. Rev. B **83**, 153413 (2011).

[14] G. Giovannetti, P. A. Khomyakov, G. Brocks, P. J. Kelly, and J. van den Brink, Phys. Rev. B **76**, 073103 (2007).

[15] The LDA band gap of graphene on Al-terminated Al_2O_3 is 178%, 780%, and 144% larger than that on O-terminated SiO_2[12], O-terminated HfO_2[13] and h-BN[14], respectively.

[16] G. Kresse and J. Furthmüller, Comput. Mater. Sci. **6**, 15 (1996).

[17] S. Grimme, J. Comput. Chem. **27**, 1787 (2006).

[18] G. Mercurio, E. R. McNellis, I. Martin, S. Hagen, F. Leyssner, S. Soubatch, J. Meyer, M. Wolf, P. Tegeder, F. S. Tautz, and K. Reuter, Phys. Rev. Lett. **104**, 036102 (2010); D. Stradi, S. Barja, C. Diaz, M. Garnica, B. Borca, J. J. Hinarejos, D. Sanchez-Portal, M. Alcami, A. Arnau, A. L. Vazquez de Parga, R. Miranda, and F. Martin, Phys. Rev. Lett. **106**, 186102 (2011).

[19] L. Spanu, S. Sorella, and G. Galli, Phys. Rev. Lett. **103**, 196401 (2009).

[20] R. Zacharia, H. Ulbricht, and T. Hertel Phys. Rev. B **69**, 155406 (2004).

[21] A. Alkauskas, P. Broqvist, F. Devynck, and A. Pasquarello, Phys. Rev. Lett. **101**, 106802 (2008).

[22] V. Barone, O. Hod, and G. E. Scuseria, Nano Lett. **6**, 2748 (2006).

[23] Pseudo H atoms are often used in surface calculations to passivate each dangling bond. In bulk α-Al_2O_3, each Al atom with 3 valence electrons is 6-fold coordinated and each O, which need 2 electrons to satisfy being full shell, is 4-fold coordinated. Thus, each Al (O) provide 3/6=0.5 (6/4=1.5) electrons to each Al-O bond. At the Al_2O_3 surface, Al atom is only 3-fold coordinated while O is 2-fold coordinated, as shown in Fig. 1. Therefore, it need three anion-like H(1.5) pseudo H atoms to passivate each Al dangling bond and one cation-like H(0.5) pseudo H atom to passivate each O dangling bond.

[24] A strain of 2% does not influence the intrinsic electronic property of graphene, as shown in S. Choi, S. Jhi, and Y. -W. Son, Phys. Rev. B **81**, 081407 (2010).

[25] J. Neugebauer and M. Scheffler, Phys. Rev. B **46**, 16067 (1992).

[26] V. E. Henrich and P. A. Cox, *The Surface Science of Metal Oxides* (Cambridge University Press, Cambridge, England, 1994).

[27] G. Renaud, Surf. Sci. Rep. **32**, 1 (1998).

[28] J. Toofan and P. R. Watson, Surf. Sci. **401**, 162 (1998).

[29] R. D. Felice and J. E. Northrup, Phys. Rev. B **60**, 16287(R) (1999).

[30] X. Wang, A. Chaka, and M. Scheffler, Phys. Rev. Lett. **84**, 3650 (2000).

[31] H. Liu, Q. Sun, L. Chen, Y. Xu, S. Ding, W. Zhang, and S. Zhang, Chin. Phys. Lett. **27**, 077201 (2010).

[32] M. Long, L. Tang, D. Wang, L. Wang, and Z. Shuai, J. Am. Chem. Soc. **131**, 17728 (2009).

[33] Y. Zhang, T. Tang, C. Girit, Z. Hao, M. C. Martin, A. Zettl, M. F. Crommie, Y. R. Shen, and F. Wang, Nature (London) **459**, 820 (2009).